Structural Eng./Earthquake Eng., JSCE, Vol. 15, No. 1, 97s—106s, 1998 April

BASIC STUDY ON SIMULTANEOUS IDENTIFICATION OF CABLE TENSION AND FLEXURAL RIGIDITY BY EXTENDED KALMAN FILTER

Hiroshi ZUI[1], Tohru NISHIKAWA[2], Yoshihiro HAMAZAKI[3] and Tohru SHINKE[4]

[1]Member of JSCE, Dr. of Eng., Professor, Dept. of Civil Eng., Setsunan University (Ikeda-nakamachi 17-8, Neyagawashi, Osaka 572, Japan)
[2]Member of JSCE, M. Eng., Shinkouzou, Ltd. (Minani-honmachi 4-5-7, Chuo-ku, Osaka 541, Japan)
[3]Member of JSCE, Ms. of Eng., Dept. of Structural Eng., KOBE STEEL Ltd. (Iwaya-nakamachi, Nada-ku, Kobe, 650, Japan)
[4]Member of JSCE, Dr. of Eng., Professor, Dept. of Civil Eng., Kobe Tech. Coll. (Gakuen-higashimachi, Nisi-ku, Kobe, 651-21, Japan)

The extended Kalman filter is applied to the simultaneous identification of the flexural rigidity and tension of cables. The equivalent one degree of freedom system is used as the mathematical model of cables on the extended Kalman filter in which the first or second mode of vibration of cables is only taken into account.

First, the calculated response values obtained by the same order model and finite element model are used and the effects of the method are confirmed. Next, the experiment is carried out by using aluminum plates instead of cable specimens and the effects of the method are examined.

Key Words : identification, flexural rigidity, cable tension, vibration method, extended kalman filter

1. INTRODUCTION

[1] During the construction of cable-supported bridges such as Nielsen bridges or cable-stayed bridges, the cable tensions must be adjusted so that cable tensions and bridge geometry may be optimized. Therefore, accurate measurement of cable tensions has practical significance and a simple, quick and reliable method of measurement is needed by the field engineers. The vibration method by which cable tensions are estimated from measured natural frequencies is utilized for the measurement of cable tensions due to its simplicity and speed. The natural frequencies of cables are influenced not only by cable tension but also by flexural rigidity, the sag-span ratio and the inclination of the cable, and these effects should be taken into account for the estimation of cable tensions.

Practical formulas for this purpose were proposed by the authors in Refs. 1) and 2). Cable tensions can easily be estimated from these formulas using measured natural frequencies of cables, and these formulas are therefore widely used. The flexural rigidity of the cable, however, must be obtained previously. Particularly when the cables used are short, the natural frequencies of cables are influenced largely by the flexural rigidity. In addition, damper facilities are often utilized for the rain vibration control of cable-stayed bridges, and the flexural rigidity values for the cable are needed to produce a design of the optimum precision[3)].

Although the flexural rigidities of cables are often needed, it is difficult to determine the exact values because they vary according to the type of cable and the tensions introduced. Up to now, static bending tests or calibration methods using measured cable tensions and natural frequencies have been utilized to estimate the flexural rigidities of cables. Recently, a new method has been proposed by which the flexural rigidities of cables

[1] This paper is translated into English from the Japanese paper, which originally appeared on J. Struct. Mech. Earthquake Eng., JSCE, No.556/I-38, pp. 189-196, 1997.1.

are estimated by the least square method, using measured natural frequencies in periodical solutions of high-frequency modes[4].

At the same time, many studies have been carried out concerning the problems of identifying the dynamic characteristics of structures on the basis of measured vibration data. These are experimental modal analyses which are useful for estimating modal parameters such as natural frequencies, modal damping, and mode shapes. They can be applied in system identification to directly estimate vibration parameters such as mass, damping and stiffness matrices. These techniques are mainly developed in the electrical or mechanical areas of control engineering.

One of these techniques is the Kalman filter, which is an algorithm of time-domain identification techniques, in which the least square estimations of state variables are calculated on the basis of measured values given for each sample time[5]. The Kalman filter consists of the state equation of a linear system. A similar algorithm can be obtained, however, even for a nonlinear system, to linearize the state equation around the reference trajectory. This algorithm is known as the extended Kalman filter, and is used in civil engineering to estimate the dynamic characteristics of structures[6].

In the study described herein, the extended Kalman filter is applied in the simultaneous identification of both the flexural rigidity and the tension of cables. It uses the measured response values obtained by forced vibration tests of cables. The equivalent one degree of freedom system is used as the mathematical model of cables on the extended Kalman filter in which the first or second mode of vibration of cables is only taken into account. Though the equation of natural frequency, cable tension and flexural rigidity thereby becomes nonlinear, the approximate formula proposed in the practical formulas of the vibration method is used on the relation between these parameters.

First, the same order mathematical model is established, assuming the flexural rigidity and tension values, and the state equation of this model is solved numerically. A finite element model with twenty beam elements is produced and solved, taking into account the pretensioned axial force effects. The calculated response values obtained by the same order mathematical model and finite element model are used as measured values by adding Gaussian white noises. Thus the method are verified. Next, the experiment is carried out, using aluminum plates instead of cable specimens, and identifications are made, using sampled time-historical responses to examine the possibility of simultaneous identification of flexural rigidity and tension. As it is difficult to produce a state vector in which flexural rigidity and tension are directly included, non-dimensional parameter-related flexural rigidity and tension are calculated, using these identified parameters. The computer program for the identification uses Fortran.

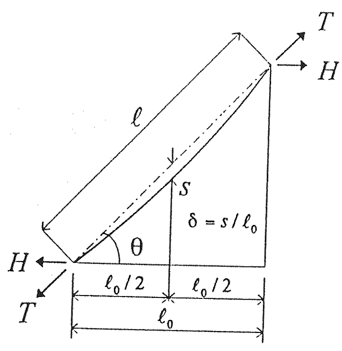

Fig. 1 Inclined cable and its features

2. BASIC EQUATIONS OF CABLE

(1) Equation for motion of cable with flexural rigidity

The equation for motion of a clamped beam with tension T is[2] :

$$\frac{\partial^2}{\partial x^2}\left(EI\frac{\partial^2 v}{\partial x^2}\right) - T\frac{\partial^2 v}{\partial x^2} + \frac{w}{g}\frac{\partial^2 v}{\partial t^2} = p(x,t) \quad (1)$$

where EI is the flexural rigidity of cable, v is deflection in $y-$ direction due to vibration, T is cable tension in the direction of OP as shown in **Fig. 1**, w is weight of cable per unit length, g is gravitational acceleration and $p(x,t)$ is distributed external force. Eq. (1) is a partial differential equation concerning time t and coordinate x.

As shown in the Fig. 1, even in cases when cable is inclined and sag exists, if the sag-to-span ratio is sufficiently low, it can be assumed that the geometric shape of cable is expressed by a parabolic formula, motion in the $x-$ direction is negligibly small and the effect of derivative cable tension due to vibration is also negligibly small for unsymmetric modes such as the second mode. In such cases, the same equation as Eq. (1) above is obtained. Therefore, if the vibration modes are limited as unsymmetric modes, Eq. (1) becomes applicable for inclined cable with sag. Eq. (1) also becomes applicable for symmetric modes when sag is very small or the order of the vibration modes is high because the effect of derivative cable tension due to vibration is negligibly small in such cases. Using the variable separation and orthogonal relations between each two modes, the equation of motion can be obtained, expressed by the modal coordinate q_n as follows:

$$\ddot{q}_n + 2\zeta_n\omega_n\dot{q}_n + \omega_n^2 q_n = \frac{p_n(t)}{m_n} \qquad (2)$$

where ζ_n is the n-th modal damping, ω_n is the n-th circular frequency, m_n is the n-th modal mass and p_n is the generalized external force for the mode shape ϕ_n. m_n and p_n are expressed as

$$m_n = \int_0^{\ell} \phi_n^2(x) m dx \qquad (3)$$

$$p_n(t) = \int_0^{\ell} \phi_n(x) p(x,t) dx \qquad (4)$$

For Eq. (2), it is assumed that Rayleigh type damping is present.

(2) Relations between natural frequencies and cable tension

Next dimensionless parameter is introduced in Reference 2) in order to obtain the relations between natural frequencies and cable tension:

$$\xi = \sqrt{\frac{T}{EI}} \cdot \ell \qquad (5)$$

ξ is a parameter concerning cable stiffness in transverse direction and when ξ is small, cable characteristics coincide with those of a clamped beam, and the larger ξ becomes, the more closely the cable characteristics begin to resemble those of string. Consequently, the effects of flexural rigidity are expressed by a single parameter ξ on the relations between natural frequencies and cable tension.

Since the equation of free vibration, concerning natural frequencies is a transcendental equation, cable tensions cannot be obtained directly from the measured frequencies. Also, the first (symmetric first) or the second (unsymmetric first) vibration modes can be easily excited artificially. Therefore, two types non-dimensional parameters are introduced in relation to the region of ξ and approximate formulas between these two parameters and ξ are obtained in Reference 2).

(i) In cases where ξ is large:

$$\eta_n = f_n / f_n^s \qquad (6)$$

where f_n is the $n-th$ natural frequency of the cable and f_n^s is the theoretical value of the $n-th$ natural frequency of a string:

$$f_n^s = \frac{n}{2\ell}\sqrt{\frac{Tg}{w}} \qquad (7)$$

(ii) In cases where ξ is small:

$$\varphi_n = f_n / f_n^B \qquad (8)$$

where ${f_n}^B$ is the theoretical value of the $n-th$ natural frequency of a beam clamped at both ends and is given as follows:

$${f_n}^B = \frac{{\alpha_n}^2}{2\pi\ell^2}\sqrt{\frac{EIg}{w}} \qquad (9)$$

where

$$\alpha_1 = 4.730 \ , \ \alpha_2 = 7.853$$

When the cable tension approaches zero($\xi = 0$), φ_n becomes 1.

Within the limit of the first and second modes, approximate solutions of the transcendental equations concerning natural frequencies can be expressed in the form[2)]

$$\eta_1 = \frac{\xi}{\xi - 2.2} \qquad (17 \le \xi) \quad (10)$$

$$\eta_1 = 1.075\sqrt{1 + \left(\frac{6.8}{\xi}\right)^2} \qquad (6 \le \xi \le 17) \quad (11)$$

$$\varphi_1 = \sqrt{1 + \frac{\xi^2}{42}} \qquad 0 \le \xi \le 6 \quad (12)$$

$$\eta_2 = 0.985\frac{\xi}{\xi - 3.1} \qquad (17 \le \xi \le 60) \quad (13)$$

$$\varphi_2 = \sqrt{1 + \frac{\xi^2}{85}} \qquad 0 \le \xi \le 17 \quad (14)$$

where Eqs. (10) , (11) and (11) are the approximate formulas for the first mode and Eqs. (13) and (14) are for the second mode. These approximate solutions agree fairly well with the exact solutions within the error of 0.4% for the each region of ξ .

3. FORMULATION OF IDENTIFICATION EQUATIONS BY EXTENDED KALMAN FILTER

(1) Mathematical model

In order to establish the extended Kalman filter as the output filter of the cable tension and the flexural rigidity by inputting the observed responses, a mathematical model of the cable is necessary to relate the input and output data.

The Kalman filter is composed of a time update algorithm, which solves equations of motion of the objective system, and an observation update algorithm, which modifies the state vector obtained by a time update, using observed values.

To set up a real time processing system on a micro computer, the dynamic characteristics of the objective system must be expressed in a mathematical model with the smallest possible degree of freedom. The responses of the cables are determined by induced forces which excite the cables and the dynamic characteristics of the cables. The mathematical model must be one which can express these characteristics. Eq. (2) is used to express the motion of cables for each vibration mode.

Eq. (2) is transformed in the following way, by using the non-dimensional parameter η_n which is the relationship between a natural frequency and the frequency of a string:

$$\ddot{q}_n+2\zeta_n\eta_n C_x\sqrt{T}\dot{q}_n+\eta_n^2C_x^2Tq_n=\frac{\phi^T}{m_n}\cdot p(x,t) \quad (15)$$

where $C_x=\dfrac{\pi n}{\ell\sqrt{m}}$

Eq. (2) is transformed in a different way, using the non-dimensional parameter φ_n , to express the relationship between a natural frequency and the frequency of a clamped beam:

$$\ddot{q}_n+2\zeta_n\varphi_n J_x\sqrt{\psi}\dot{q}_n+\varphi_n^2{J_x}^2\psi q_n=\frac{\phi^T}{m_n}p(x,t) \quad (16)$$

where $\psi = EI/EI_0$, EI_0 = the theoretical flexural rigidity of prismatic section of cable, $J_x=\dfrac{{\alpha_n}^2}{\ell^2}\sqrt{\dfrac{EI_0}{m}}$.

Eq. (15) is used for the region $\xi > 6$ for the first mode and $\xi > 17$ for the second mode. Eq. (16) is used for the region $\xi \leq 6$ for the first mode and $\xi \leq 17$ for the second mode.

In order to apply the Kalman filter, the equation of motion, (15) or (16) is transformed into the state-space form as follows:

$$\dot{\boldsymbol{x}}=\boldsymbol{A}\boldsymbol{x}+\boldsymbol{b}p(x,t) \quad (17)$$

where

$$\boldsymbol{x}=\{q_n,\dot{q}_n\}^T$$

$$\boldsymbol{A}=\begin{bmatrix}0 & 1\\ -\eta_n^2C_x^2T & -2\zeta_n\eta_nC_x\sqrt{T}\end{bmatrix} \quad (18)$$

or

$$\boldsymbol{A}=\begin{bmatrix}0 & 1\\ -\varphi_n^2J_x^2\psi & -2\zeta_n\varphi_nJ_x\sqrt{\psi}\end{bmatrix} \quad (19)$$

$$\boldsymbol{b}=\left\{0,\frac{\phi}{m_n}\right\}^T \quad (20)$$

In solving Eq. (17), the discrete time representation by discrete time interval, Δt , becomes

$$\boldsymbol{x}_{i+1}=\boldsymbol{\Psi}\,\boldsymbol{x}_i+\boldsymbol{B}\,p(x,t) \quad (21)$$

where

$$\left.\begin{aligned}\boldsymbol{\Psi}&=e^{\boldsymbol{A}_i\Delta t}=\sum_{k=0}\frac{(\Delta t)^k}{k!}(\boldsymbol{A}_i)^k\\ \boldsymbol{B}&=\sum_{k=0}\boldsymbol{b}\frac{(\Delta t)^{k+1}}{(k+1)!}(\boldsymbol{A}_i)^k\end{aligned}\right\} \quad (22)$$

Eq. (21) is a solution of (17) and is an equation for prediction which can predict the state vector at step $(i+1)$.

(2) The design of the extended Kalman filter

Using the state-space equation and its solutions derived in the previous section, the equations of the extended Kalman filter are represented to predict the parameters for damping, natural frequencies and the cable tension.

In order to estimate any unknown parameters included in the state-space equation, the state vector is extended to include the unknown parameters.

The unknown parameters are the following three parameters:

In cases where the natural frequencies of the string are used, ζ_n, η_n and $\sqrt{T}$ are the unknown parameters, and the extended state vector is defined as:

$$\boldsymbol{Z}_i=\left\{q_n,\dot{q}_n,\zeta_n,\eta_n,\sqrt{T}\right\}^T \quad (23)$$

In cases where the natural frequencies of the clamped beam are used, ζ_n, φ_n and $\sqrt{\psi}$ are the unknown parameters, and the extended state.vector is defined as:

$$\boldsymbol{Z}_i=\left\{q_n,\dot{q}_n,\zeta_n,\varphi_n,\sqrt{\psi}\right\}^T \quad (24)$$

The coefficient matrices of Eqs. (18) and (19) are expressed as functions of the extended state vector, $\boldsymbol{Z}_i$, defined by Eqs. (23) and (24) .

Substituting these equations into Eq. (22), $\boldsymbol{\Psi}$ and $\boldsymbol{B}$ are obtained and all of their components become a function of the unknown parameters included in the extended state vector $\boldsymbol{Z}_i$. Consequently, they must be recalculated at each time of observation update.

The prediction equation of $\boldsymbol{Z}_{i+1}$ becomes

$$\boldsymbol{Z}_{i+1} = \begin{bmatrix} \boldsymbol{\Psi} & \mathrm{o} \\ \mathrm{o} & \boldsymbol{I} \end{bmatrix} \boldsymbol{Z}_i + \begin{Bmatrix} \boldsymbol{B} \\ \mathrm{o} \end{Bmatrix} p(x,t) + \begin{Bmatrix} \boldsymbol{w}_i \\ \hat{\boldsymbol{w}}_i \end{Bmatrix} \tag{25}$$

where $\boldsymbol{w}_I$ and $\hat{\boldsymbol{w}}_i$ are Gaussian white noise expressing the system noise of the state vector. Eq. (25) is rewritten as

$$\boldsymbol{Z}_{i+1} = \quad \boldsymbol{\Phi}(\boldsymbol{Z}_i) + \boldsymbol{G}p(x,t) + \boldsymbol{W}_i \tag{26}$$

The time update algorithm for the extended Kalman filter yields the following derivations from Eq. (26) :

$$\hat{\boldsymbol{Z}}_{i+1/i} = \quad \boldsymbol{\Phi}(\hat{\boldsymbol{Z}}_{i/i}) + \boldsymbol{G}p(x,t) \tag{27}$$

$$\boldsymbol{P}_{i+1/i} = \quad \boldsymbol{\Upsilon}_{i/i}\boldsymbol{P}_{i/i}\boldsymbol{\Upsilon}_i^T + \boldsymbol{Q}_i \tag{28}$$

$$\boldsymbol{\Upsilon}_i = \quad \partial\boldsymbol{\Phi}(\hat{\boldsymbol{Z}}_{i/i})/\partial\hat{Z}|_{\hat{Z}=\hat{\boldsymbol{Z}}_{i/i}} \tag{29}$$

where, $\boldsymbol{P}$ is the error co-variance matrix of the predicted state vector and $\boldsymbol{Q}$ is the error co-variance matrix of the system noise, $\boldsymbol{W}_i$.

The observation update algorithm is next derived . The observation vector, $\boldsymbol{y}$, is related to the state vector, $\boldsymbol{Z}$, as follows:

$$\boldsymbol{y}_i = \boldsymbol{h}(\boldsymbol{Z}_i) + \boldsymbol{v} \tag{30}$$

where, $\boldsymbol{v}$ is Gaussian white noise expressing observation error.

The observation update algorithm is given by the conditions which minimize the errors of estimated state quantities :

$$\hat{\boldsymbol{Z}}_{i/i} = \quad \hat{\boldsymbol{Z}}_{i/i-1} + \boldsymbol{K}_i\{\boldsymbol{y}_i - \boldsymbol{h}_i(\hat{\boldsymbol{Z}}_{i/i-1})\} \tag{31}$$

$$\boldsymbol{K}_i = \quad \boldsymbol{P}_{i/i-1}\boldsymbol{H}_i^T\{\boldsymbol{H}_i\boldsymbol{P}_{i/i-1}\boldsymbol{H}_i^T + \boldsymbol{R}_i\}^{-1} \tag{32}$$

$$\boldsymbol{P}_{i/i} = \quad \boldsymbol{P}_{i/i-1} - \boldsymbol{K}_i\boldsymbol{H}_i\boldsymbol{P}_{i/i-1} \tag{33}$$

where,

$$\boldsymbol{H}_i = \quad \partial\boldsymbol{h}(\boldsymbol{Z}_i)/\partial\boldsymbol{Z}_i|_{Z=\hat{\boldsymbol{Z}}_{i/i}} \tag{34}$$

$\boldsymbol{K}_i$ is the Kalman gain matrix, which minimize the errors in the estimated state quantities and $\boldsymbol{R}$ is the error co-variance matrix of the observation noise.

In all these equations, the subscript $i/i-1$ denotes a quantity evaluated at instant i based on observation at instant $i-1$.

Calculations of (29) and (34) are very complicated and it is almost impossible to calculate by manual operations if more than three polynomial terms are taken in Eq.(22).

Multiplication of polynomial (22) and the differential calculus of Eqs. (29) and (34) are carried out by MAPLE[8] which is one of the symbolic and algebraic manipulation languages, which has FORTRAN codes incorporated into its program.

The four polynomial terms are adopted in Eq. (22) .

The initial conditions are given as follows:

$$\hat{Z}_{0/-1} = \bar{\boldsymbol{Z}}_0, \qquad \boldsymbol{P}_{0/-1} = \boldsymbol{\Sigma}_0 \tag{35}$$

where $\bar{\boldsymbol{Z}}_0$ is the mean value of the initial estimate of the state and $\boldsymbol{\Sigma}_0$ is the initial estimate of the error co-variance matrix for the system noise of the state.

Since the accuracy of the time update calculations depends upon the incremental time step of integration, the time update calculations are carried out by one-tenth of the time step of the observation update. Also, if the calculations for Eqs. (27) $\sim$ (29) , and Eqs. (31) $\sim$ (34) are carried out under the original form, some numerical instability may occur. Some algorithms have been proposed to improve these numerical instability. Among these, the numerically most stable method is the UD decomposition algorithm, which utilizes the symmetric non-positive characteristics of the co-variance matrix $\boldsymbol{P}$[5]. The UD decomposition algorithm is what is used in this study.

The approximate formulas, such as Eqs. (10) $\sim$ (14) concerning transverse rigidity, with the terms ξ and η_n or φ_n are used when the flexural rigidity and axial force are calculated from the identified state.

4. NUMERICAL STUDY

(1) When using a mathematical model of the same-order

The simulation program is implemented on the basis of the time update algorithms, Eqs. (27) $\sim$ (29) , and the observation update algorithms, Eqs. (31) $\sim$ (33). Verification is then carried out using the following process.

1) Assuming the exact values of the cable tension T , the damping coefficient ζ, the nondimensional parameter ξ , and the flexural rigidity EI of the model, the state equation (17) is solved by the fourth-order Rungqutta-Gill method. Response values such as displacements, velocities or accelerations are obtained from these results, and adding quasi-Gaussian white noise which values are several % of the response values, and these values are used as observed values.

2) Assuming appropriate initial values, the identification algorithm is applied to the above observed values, and the exact values of EI and T are estimated.

Table 1 Cable properties used in verification

ℓ	$5.0m$	Diameter	$4.6cm$
mg	$13.03\ tf/m$	EI	$1.758tf \cdot m^2$
ζ_1	0.03	EL_0	$3.510tf \cdot m^2$

Table 2 Cable tension T and flexural rigidity ξ

Case	$T\ (tf)$	ξ	$f_1\ (Hz)$	η_1 or φ_1
(a)	24	18.5	15.2	$\eta_1 = 1.135$
(b)	2	5.33	6.71	$\varphi_1 = 1.295$
(c)	1	3.77	5.99	$\varphi_1 = 1.157$

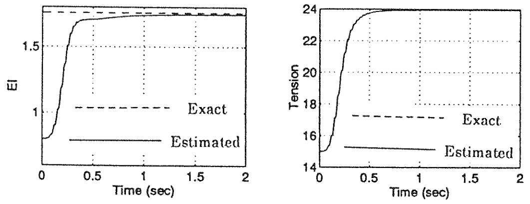

Flexural rigidity(EI) Tension(T)

Fig. 2 Evolution of estimated parameters on the same-order mathematical model $\xi = 18.5$

The time increment for the observation update is 0.01 second. Table 1 shows the cable properties used in the verification. The cable tension (nondimensional transverse rigidity, ξ) is changed in three steps, as shown in Table 2.

A simulation is carried out, assuming the initial values of cable tension, damping coefficient and flexural rigidity to be half or twice the exact value.

The sinusoidal wave which frequency is the same as the first natural frequency is used as the exciting force. The amplitude is 2.0 kgf and the force is applied at the center of the span ($\ell/2$). The response accelerations at the points of ($\ell/2$) and ($\ell/4$) are used as observed values.

Fig. 2 provides an example of the evolution of the estimated cable tension (T) and flexural rigidity (EI). The estimated values closely approach the exact values and the validity of the identification algorithm is confirmed.

Table 3 shows the estimated results of the cable tension (T) and the flexural rigidity (EI).

Cable tension and flexural rigidity can be estimated with sufficient accuracy from the characteristics of the cable which are similar to those of strings and to those of beams, in cases where the same order mathematical model is used.

Table 3 Estimated results for cable tension(T) and flexural rigidity(EI)using a same-order mathematical model

Case	Parameter	Exact values	Estimated values	Ratio
(a)	EI	1.758	1.745	0.993
	T	24.00	23.93	0.997
(b)	EI	1.758	1.760	1.001
	T	2.000	1.998	0.999
(c)	EI	1.758	1.749	0.995
	T	1.000	1.002	1.002

(2) In cases where the solutions of the finite element model are used

The same model with Table 1 is expressed by the finite element model divided into twenty elements and the same tension with Table 2 is introduced. Considering the geometric stiffness due to the cable tension, the response values are calculated under the same conditions with the same-order mathematical model. After adding quasi-Gaussian white noise which values correspond to several % of the response values, these values are used as the observed values. Damping is given as $C/K = 2\zeta_1/\omega_1$.

First, the first natural frequency calculated by the finite element method is compared with the theoretical value of a beam with axial force,.and the coincidence of these values is confirmed. The response values of the finite element model are calculated on the same exciting condition. Then these values added quasi-Gaussian white noise are used as the observed values. After that, the unknown variables are identified under the same initial and observation conditions as in the previous section. Fig. 3 shows an example of the evolution of the estimated cable tension(T) and flexural rigidity(EI).

In the response values of the finite element method, the higher modes are a little excited. These components are not considered in the model of the extended Kalman filter and the accuracy of the identification declines slightly in comparison with the results of a mathematical model of the same order.

Table 4 shows the estimated results for cable tension (T) and flexural rigidity (EI) . Cable tension and flexural rigidity are estimated fairly well from the characteristics of cable which are

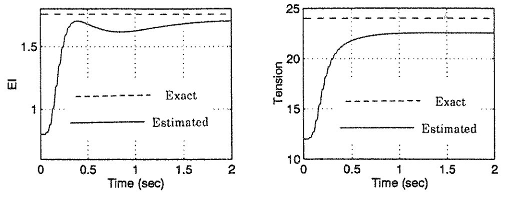

Flexural rigidity(EI) Tension(T)

Fig. 3 Estimated results for cable tension(T) and flexural rigidity(EI) using the finite element model $\xi = 18.5$

Table 4 Estimated results for cable tension(T) and flexural rigidity(EI) using the finite element model

Case	Parameter	Exact values	Estimated values	Ratio
(a)	EI	1.758	1.703	0.97
	T	24.00	22.56	0.94
(b)	EI	1.758	1.723	0.98
	T	2.000	1.882	0.94
(c)	EI	1.758	1.704	0.97
	T	1.000	0.943	0.94

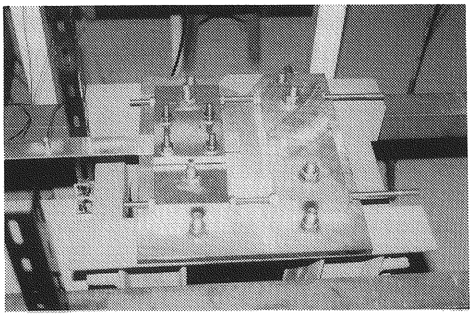

Photo 1 Device for clamping specimens

similar to those of strings and those of beams, when the finite element method is used.

5. EXPERIMENTS USING ALUMINUM PLATES (AS SPECIMENS)

(1) Equipments used for the experiments

The experimental equipments consist of the device for clamping the ends of the specimens and adjusting the axial forces, and an experimental stand (**Phote 1**),(**Phote 2**).

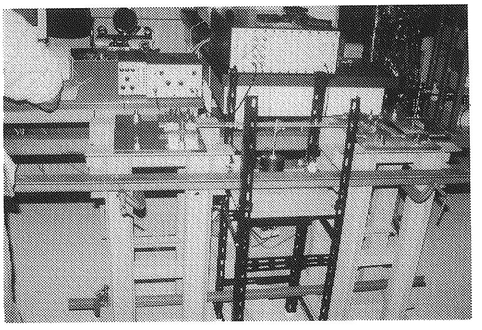

Photo 2 An experimental stand

Table 5 Properties of specimens used in experiments

Specimen	ℓ (mm)	Width (mm)	Height (mm)	I (mm^4)
AL1	500	29.97	3.0	67.5
AL2	800	30.00	2.0	20.0

(2) Specimens

Aluminum plates are used as specimens because their flexural rigidity is definite. **Table 5** shows the properties of specimens.

(3) Excitation tests

The specimens were positioned horizontally and were excited sinusoidally in the first or second mode of vibration by a small electromagnetic oscillator. The exciting force was measured by the force sensor attached at the top of the exciting rod. Piezo-electric accelerometers were used as sensors for the measurement of the response values. Though the size of the accelerometer was very small, its mass was not negligible in comparison with that of the aluminum plate. Therefore, the five sensors were attached at equal intervals in order to get a nearly uniformly distributed mass.

The main purpose of the test is to verify the possibility of identifying the axial force and flexural rigidity for cables with characteristics similar to those of beams and strings. Consequently, the axial forces are adjusted so as to satisfy the conditions of ξ ; $\xi \leq 6$ or $6 \leq \xi$.

First, the natural frequencies of vibration modes of the first to third mode were obtained by experimental modal analysis for specimens without tension. These frequencies were substituted

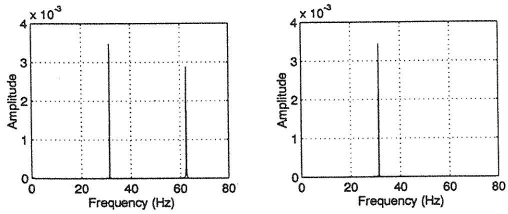

(a) Raw data (b) Filtered data

Fig. 4 Fourier spectrum of experimental data

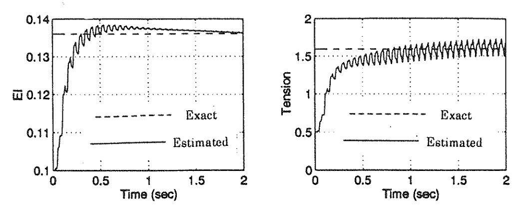

Flexural rigidity (EI) Tension(T)

Fig. 5 Evolution of estimated parameters using raw experimental data ($\ell = 800, \xi = 2.74$)

Table 6 Specimen mass obtained by experimental modal analysis

Specimen	f_1^B (c/s)	m $(kgf \cdot mm/s)$
Al1	39.43	5.99×10^{-8}
Al2	15.65	1.72×10^{-8}

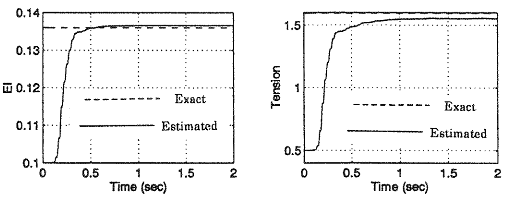

Flexural rigidity(EI) Tension(T)

Fig. 6 Evolution of estimated parameters using filtered data ($\ell = 800, \xi = 2.74$)

into (9) as the natural frequencies of the clamped beam without axial force, f_n^B , and the mass of the specimen per unit length, m , was obtained by the reverse calculation using the value of EI. The mass of the sensors was included in the m.

Next, the specimens were pulled to tension by the clamping device, and the axial force was gradually increased in order to satisfy each of the conditions, $\xi \leq 6$ and $6 \leq \xi$. Exciting tests were carried out for each condition.

As the measured data include higher mode components which are not taken into account in the mathematical model, the filtered data which were passed through a band-pass filter were also used for the identification data along with the raw data.

Fig. 4-(a) shows an example of the spectrum for the raw data, while **Fig. 4**-(b) shows the spectrum for the filtered data. A digital filter (IIR) was used for band-pass filter.

(4) Experimental verification using the excitation test data

The mass values obtained by the reverse calculations using the value of EI and the measured first natural frequency of the specimen without tension $f_1{}^B$ are shown in **Table 6**. The mass value of a specimen Al1 is larger than that of a specimen Al2 because of the larger plate thickness and the contribution of sensor mass per unit length. The vertical accelerations at the points $\ell/2$ and $\ell/4$ were measured at a constant sampling time interval, $\Delta t = 1/256$ sec. The total sampling time was $t = 4sec$ and the number of each type of data was 1024. **Fig. 5** shows an example of the estimated results for cable tension (T) and flexural rigidity (EI) in cases where raw data were used. When raw experimental data are used, the estimated values oscilate around the exact value and are not stable. The reason for this may be that raw experimental data include higher mode components which are not taken into account by the extended Kalman filter.

Fig. 6 provides an example of the estimated results for tension (T) and flexural rigidity (EI) in cases where filtered data were used.

The estimated values approximate the exact values much more closely and with much greater stability than where raw data are used, and the accuracy of the identification is much greater.

Table 7 shows the estimated results based on experimental data for cable tension (T) and flexural rigidity (EI) . The estimated values agree fairly well with the exact values in both cases where raw data were used and where filtered data were used, when the data were nondimensionalized by the natural frequency of the clamped beam $\xi \leq 6$ or by the natural frequency of the string $\xi > 6$.

Table 7 Estimated results for cable tension (T) and flexural rigidity (EI) using experiment results

Specimen	ξ	EI / T	Exact values	Estimated values	
				Raw data	Filtered data
Al1	5.21	EI	4.59×10^5	4.37×10^5	4.40×10^5
		T	49.8	53.7	52.9
	13.4	EI	4.59×10^5	4.46×10^5	4.59×10^5
		T	330.2	332.5	330.1
Al2	2.74	EI	1.36×10^5	1.36×10^5	1.36×10^5
		T	1.59	1.66	1.59
	11.32	EI	1.36×10^5	1.35×10^5	1.34×10^5
		T	27.2	27.4	27.3
	19.1	EI	1.36×10^5	1.49×10^5	1.48×10^5
		T	77.3	75.5	75.3

6. CONCLUSIONS

This study proposes a method of identification, based on an extended Kalman filter, for simultaneously estimating the cable tension and the flexural rigidity of cable. The conclusions reached in the study can be summarized in the following points.

Cable tension and flexural rigidity can be estimated with sufficient accuracy from the characteristics of cable which are similar to those of strings and those of beams when the same-order mathematical model is used.

The estimated values for axial force and flexural rigidity agree fairly well with the exact values when the response values of the finite element method are used.

The studies confirmed expectations that the axial force and the flexural rigidity could be estimated with quite good accuracy on the basis of cable characteristics similar to those of strings and of beams, when the experimental data are obtained by means of an excitation test on an aluminum plate.

The accuracy of the identification is better when filtered data are used than when raw data are used. The reason may be that the model of the extended Kalman filter is based on a single degree of freedom, while the raw data obtained from the excitation test include higher mode components.

In this study, sinusoidal excitation forces were applied. Use of an impulse hammer for the force excitation makes the excitation tests easier and more convenient. Higher mode components are, however, included in the excitation forces and response values for the impact tests and these values must be run through a band-pass filter. It can be expected that the components of higher frequencies will be predominant in both the excitation forces and the response values. There still remain some questions concerning whether or not it is possible to extract the specific lower component with sufficient accuracy by means of the band-pass filter. It may be necessary to consider extending the study with plural components. This would be the subject for a future study, along with the verification of the present method using actual cables. It is hoped that this research will further advance the study of applications of robust control theory which will make it possible to weigh a specific region in the frequency domain.

ACKNOWLEDGMENT : This study was supported by a grant from the Japanese Ministry of Education (Project Number 07650557, H. Zui, Principal investigator).

REFERENCES

1) Shinke,T.,Hironaka,K., Zui,H. and Nishimura,H.: Practical formulas for estimation of cable tension by vibration method Proc., of Japanese Society of Civil Engineers, No. 294, pp. 25-34, 1980. (in Japanese)
2) Zui,H., Shinke,T. and Namita,Y. : Practical formulas for estimation of cable tension by vibration method Journal of Structural Engineering, American Society of Civil Engineers, Vol.122, No. 6, pp. 651-656, 1996.
3) Yoneda,M., Utsumi,Y. and Iseki,J.: JSCE Journal of Structural Engineering, Vol.40A, pp.883-895, 1994. (in Japanese)
4) Yamagiwa,I., Utsuno,H., Sugano,N. and Sugii,K. : Vibration method to estimate flexural rigidity of cable and cable tension at one time, , JSCE Journal of Structural Engineering, Vol.42A,pp 547-554. 1996. (in Japanese)
5) Katayama,T. : Applied Kalman Filter, Asakura, 1983. (in Japanese)
6) Hoshiya,M. and Saitou,E. : Identification problem of some seismic systems by extended Kalman filter, Proc. of the Japanese Society of Civil Engineers, No. 339, pp.20-33, 1983. (in Japanese)
7) Shimada,T. : Estimating method of cable tension from natural frequency of high mode, Proc., of the Japanese Society of Civil Engineers, No. 501 ／I-29, pp.163-171 , 1994.(in Japanese)
8) The Math Works Inc. : Symbolic Math Toolbox User's Guide for Use with MATLAB, 1993.